Journal of Rare Cardiovascular Diseases



RESEARCH ARTICLE

Allosteric Inhibition of PTP1B by Substituted Thiazolidine-2,4-diones: Design, Molecular Docking, Synthesis, ADMET Prediction and In-vitro Enzyme Inhibition Assay

Shubham V Pawar^{1*}, Gaurav R Rane¹ and Anagha M Joshi¹

¹Department of Pharmaceutical Chemistry, SCES's Indira College of Pharmacy, Savitribai Phule Pune University, Pune.

*Corresponding Author Shubham V Pawar (svpawar127@gmail.com)

Article History
Received: 04/08/2025
Revised: 19/08/2025
Accepted: 09/09/2025
Published: 26/09/2025

Abstract: PTP1B is a major phosphatase responsible for dephosphorylation of many substrates involved in metabolic disorders. It has proven to be validated target for many disorders such as T2DM, obesity, and cancer etc. The active site of this enzyme was an area for many researchers for the last 2-3 decades. But due to very conservative active site a problem in selectivity and permeability become hurdles in the development of inhibitors. The allosteric site has also proven to inhibit the activity of enzyme. The FBDD approach was implemented to design new inhibitors. The 3,5 disubstituted thiazolidine-2,4-dione derivatives were synthesized and subjected various in-silico and in-vitro analysis. In molecular docking studies compound 5 have given the lowest docking score and shown better binding with the allosteric site of enzyme. whereas other derivatives (6-18) have also showed good binding affinity with different types of interaction such as H-bonding, Salt bridges, and hydrophobic interactions with different amino acids of binding site. The drug likeliness and pharmacokinetic properties along with ADMET parameters of all the compounds were found to be satisfactory. The outcomes of in-vitro enzyme inhibition assay are given in the form of IC50 values ranges from 4.14±1.01 to 105.10±0.30. All the designed compounds have shown inhibitory activity against PTP1B enzyme. Compound 7 had least IC50 value of 4.14±1.01 followed by compound 12 $(5.25\pm0.48 \mu M)$ & 9 $(15.20\pm1.01\mu M)$.

Keywords: FBDD, PTP1B, Allosteric Inhibition, Molecular Docking, ADMET.

INTRODUCTION

Protein tyrosine phosphatases (PTPs) are a class of enzymes comprises of 107 enzymes. These phosphatases execute dephosphorylation by withdrawal of phosphate group in protein. (Alonso et al., 2004 & Barford et al., 1996) The phosphorylation of intracellular protein was regulated by PTP enzymes. (Barr et al.,2010) Protein tyrosine phosphatase 1B (PTP1B) is one of the enzymes from PTP class having molecular weight 35 kDa. This protein was found in various tissues, but the first PTP enzyme for human s was found from placenta. (Tonk et al., 1988) PTP1B is involved in numerous signal transduction pathways as a dephosphorylating enzyme. (Elchebly et al., 1999; Klaman et al., 2000 & Zabolotny et al., 2002) PTP1B is enzyme that causes significant deregulation of many metabolic pathway such insulin and leptin signalling pathways which shows impact on metabolism of both glucose and lipid. (Montalibet et al., 2007)

PTP1B enzyme is comprises of 435 amino acids divided in three segments out of which one is the N-terminal catalytic domain (residues 1–300), second one a regulatory region (residues 300–400), and third one indicates a C-terminal (residues 400–435). (Barford et al., 1994 & Frangioni et al.) The activity of PTP1B is modulated by various post-translational modifications, including the phosphorylation of serine and tyrosine residues within its catalytic and transmembrane domains, oxidation of Cys215 by reactive oxygen species, and the

spatial separation from its plasma membrane-localized substrates. (Dube et al., 2005).

Furthermore, PTP1B is implicated in several human including cancer, diabetes, obesity, highlighting its importance as a negative regulator in insulin and leptin signalling. It has also shown connections to Rett syndrome. (Krishnan et al., 2015) The significance of this enzyme has led to a considerable increase in research focused on positioning PTP1B as a potential therapeutic target for type 2 diabetes and obesity, as well as the creation of small molecule inhibitors of PTP1B for treatment. (Zhang & Lee, 2003) advancements in medicinal particularly in structure-based drug design (SBDD), have successfully identified numerous effective PTP1B inhibitors. Despite these efforts, translating PTP1B inhibitors into viable therapeutic drugs has largely been unsuccessful. This challenge arises primarily from the highly conservative and cationic characteristics of the PTP1B catalytic site. Most existing inhibitors utilize pTyr mimetics that bind to this catalytic site, yet they typically exhibit poor selectivity for PTP1B and lack sufficient in vivo efficacy due to their low cellular permeability. (Bar et al., 2010; Comb et al., 2010; Lee et al., 2007 & Nichols et al., 2006)

The non specificity of active site directed inhibitors to structurally similar protein can result in adverse effects within the cells (DeDecker, 2000). Additionally, these phosphatase enzymes have highly polar active sites, and

the inhibitor of these site faces problems with bioavailability (Hardy and Wells, 2004; Zhang, 2001). Due to these difficulties, it is an ultimate necessity to identify novel PTP1B inhibitors which work for other site except active sites. Allosteric site is one where small molecule inhibitors can hinder the movement of PTP1B's catalytic loop. This restriction in mobility stabilizes the enzyme in inactive form and prevents it from becoming active. This allosteric site stands out due to its non-conservative and electronically neutral nature, suggesting that targeting it could be a promising approach for achieving both selectivity and efficacy. (Wiesmann et al., 2004)

Despite extensive research, no active-site inhibitors for PTP1B have made their way into clinical practice, which has led some to deem PTP1B as 'undruggable'. On the other hand, an allosteric inhibitor that targets a less-conserved and less-polar surface area offers a promising alternative, potentially overcoming the challenges faced by active-site inhibitors. (Wiesmann et al., 2004). In this study, the Fragment based drug design along with molecular docking was used to explore the allosteric site for new inhibitors.

MATERIALS AND METHODS:

2.1 In-silico drug design:

Many crystals structure for PTP1B enzyme are available bound to differentiated ligands. In this study we have selected 1T49, a specific PDB considering the inhibition at allosteric site. (Weismann *et al.*, 2004). This same protein was used for further *in-silico* studies. The *in-silico* studies were performed using Schrodinger software version 2021-2.

The protein preparation module was used to pre-process the protein structure obtained from RCSB. The addition of missing hydrogen, removal of water molecules beyond 5 Å and assignment of appropriate bond orders were performed. The missing residues in the crystal structure was added by using prime module in protein preparation wizard. Further the crystal structure was subjected to energy minimization considering 0.3 Å RMSD as cut-off value. This protein structure was also used for grid generation, validation of grid parameters and molecular docking.

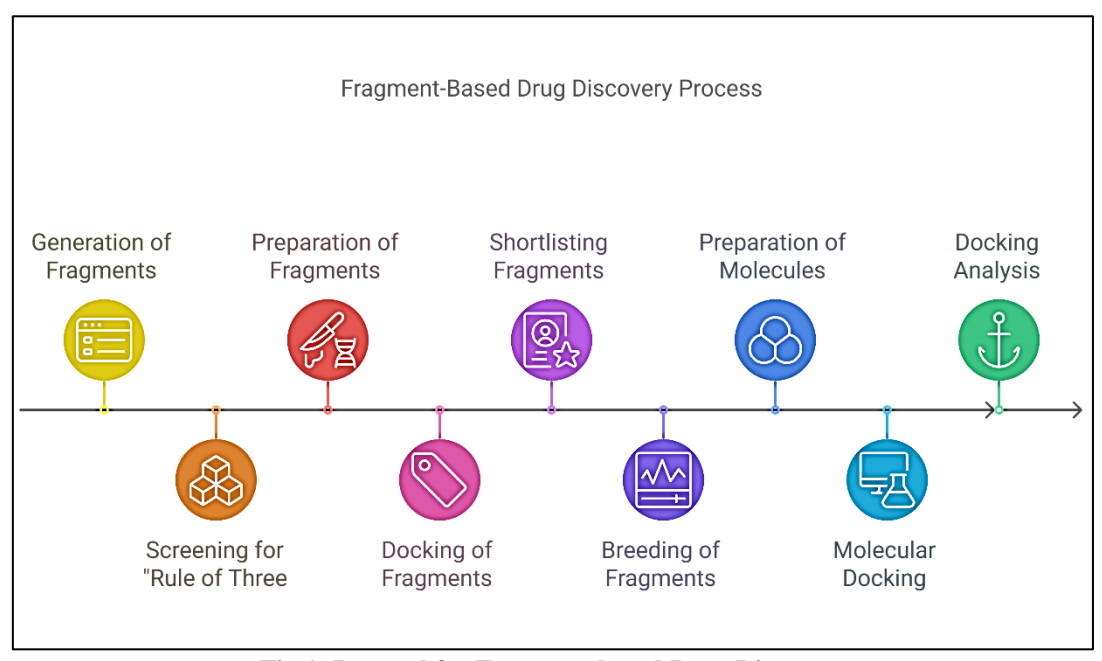


Fig 1: Protocol for Fragment-based Drug Discovery

The allosteric site of the enzyme was identified using co-crystal ligand position. The selected and pre-processed PBD (Id:1t49) was used for grid generation. The module "Receptor Grid Generation" was used to form definite grid in the interactive region considering the co-crystal ligand as grid of the centre. The inner box of the grid was fixed to 10 Å whereas outer box was fixed at 25 Å. The grid parameter validation was performed by redocking the available co-crystal ligand using new grid parameters and position of new docking with co-crystal ligand. Same validated grid was further used for all molecular docking studies.

2.1.1 Fragment based drug design:

a. Fragment screening

In FBDD, the small molecular weight fragments were used to design a new chemical entity that can inhibit PTP1B enzyme. For the generation of fragment library, various inhibitors of PTP1B enzyme had been selected, and the fragments of these



inhibitors were generated using fragment_(nameofmoleculefile).py command using powershell of Schrodinger software. (Lotfi et al., 2023; Patel et al., 2021) The above generated fragments were screened for "Rule of Three" (Najjar et al., 2019) and prepared for docking using LigPrep module (Friesner et al., 2006). These prepared ligands were used for molecular docking. The standard Precision (SP) mode of glide module was used for molecular docking calculations. Module was set to give 8 best poses of each fragment. The molecular docking was performed using OPLS_2005 Force field along with all default parameters. (Shivakumar et al., 2010)

b. Fragment joining and de novo compound design:

Analysis of fragment binding was performed using molecular docking method. The fragments having docking score < -6.0 in SP mode of docking were considered for further design process. The overlap structure of the compound was identified with their binding to the important amino acids. The prepositioned fragments in the allosteric site of PTP1B enzyme was then joined using Breed Module. This panel helps to join the available fragments by using different position and suitable bonds that can fit the fragments. Further the formed atoms were subjected to energy minimization. The newly designed molecules were ready for further study. (Patel et al., 2020; Patel et al., 2021)

2.1.2 Molecular docking:

The molecular docking of all the prepared molecules were performed using glide module of Schrodinger. The grid used for this docking study is same as one used for fragment docking. The Standard precision mode of molecular docking was used here to dock all these prepared molecules. 16 best poses were generating for each designed molecule. The default docking parameter with OPLS_2005 force field was used in the study. The molecules which have given better docking score, binding to desired amino acids and have synthetic accessibility were selected for further derivatization using site map of the allosteric site. (Zhong et al., 2009; Zhu et al., 2014; Greenwood et al., 2010)

2.1.3 Site map and derivatization of selected molecule:

The site map of the allosteric site was generated using site map module of Schrödinger where it has given idea about the hydrophobic region, hydrogen bond acceptor region and hydrogen bond donor region. The basic scaffold was evaluated by keeping the site map in consideration and the further derivatization for better binding of the molecule was performed considering the binding areas of the enzyme. Around 48 derivatives were designed using different substituted benzaldehydes and further considered for molecular docking. (Patel et al., 2020; Patel et al., 2021)

2.1.5 Ligand Preparation and Molecular docking

All the above ligands were prepared using LigPrep. The molecular docking of all the prepared molecules was performed using glide module of Schrodinger. The grid used for this docking study is same as one used for fragment docking. The Standard precision mode of molecular docking was used here to dock all these prepared molecules. 16 best poses were generating for each designed molecule. The default docking parameter with OPLS_2005 force field was used in the study. The molecules which have given better docking score, binding to desired amino acids and have synthetic accessibility were selected for further derivatization using site map of the allosteric site. (Friesner et al., 2006; Zhong et al., 2009; Zhu et al., 2014; Greenwood et al., 2010)

2.1.6 Evaluation of physicochemical, drug likeliness and pharmacokinetic properties and synthetic accessibility

pkCSM servers were employed to calculate the drug like properties and predict the physicochemical and pharmacokinetic (absorption, distribution, metabolism, excretion and toxicity) properties of all the new molecule hits selected in the previous section. A synthetic accessibility score was also predicted for each molecule from SwissADME server (Daina et al., 2017). It was found that no violation of drug likeliness rules was reported, 14 best molecules were selected based on their binding and ADMET properties. (Lipinski et al., 1997; Ertl et al., 2000; Vistoli et al., 2008; Patel et al., 2020)

2.2 Chemistry:

Starting materials and reagents were procured from local supplier and were used without further purification. The progress was monitored using thin-layer chromatography (TLC) on pre-coated silica gel F254 (Merc). Melting points determination was performed by one end open capillaries on a digital auto melting /boiling point apparatus and are uncorrected. Throughout the process, dry solvents were employed. For the NMR analysis, both 1H and 13C spectra were recorded on a Bruker Avance III HD NMR 500 MHz spectrometer. CDCl3 or DMSO-d6 served as the solvent, with TMD as the internal standard. The chemical shifts (δ) for the 1H and 13C NMR spectra are reported in parts per million (ppm), referencing the residual solvent line as the internal standard. Mass spectra were collected using a Bruker Impact HD Mass spectrometer. NMR and Mass Spectrometry were performed at Central Instrumentation Facility, Savitribai Phule Pune University, Pune, India.

The synthesis of proposed molecules (5-18) was performed using scheme 1. The basic scaffold thiazolidine-2,4-dione (3) was synthesized by condensation of chloroacetic acid (1) and thiourea (2) followed by hydrolysis.



This thiazolidine-2,4-dione (3) had further reacted with 4-nitro benzyl bromide in presence of base to given 3-(4-nitrobenzyl) thiazolidine-2,4-dione (4).

Scheme 1: Synthesis of 3,5 disubstituted thiazolidine-2,4-dione. a) i) Water, Stir ii) Conc HCl, Reflux, 10-12hrs b) DMF, K2CO3, Stirr (2-3hrs) c) Ethanol, Aldehyde, Piperidine, Gla. CH3COOH (5-7 Hrs.)

This second step product undergoes Knoevenagel condensation with different aldehyde derivatives which further get condensed at 5th C to generate 3,5 disubstituted thiazolidine-2,4-dione (**5-18**).

Step 1: Synthesis of thiazolidine-2,4-dione (3)

Chloroacetic acid **1** (1mmol) was dissolved in 6 mL of water. To this solution a solution of 1mmol of thiourea **2** dissolved in 6 mL water were added dropwise. The contents were stirred using a magnetic stirrer for 30-45 mins till the white precipitate was obtained. Concentrated HCl was added to the above suspension till white precipitates get dissolved in the solution which was then refluxed at 100-110 °C for 10-12 hrs. The final colorless needle shaped crystalline product of thiazolidine-2,4-dione **3** was obtained by cooling the reaction mixture. The reaction was monitored by TLC (MP: Chloroform Methanol (8:2). The purification of thiazolidine-2,4-dione **3** was done by recrystallization in hot ethanol. (Pattan *et al.*, 2009) 3: White colour; ¹H NMR (**500** MHz, DMSO) δ 12.4 (s,1H), 4.1 (s, 2H) **13C** NMR (**126** MHz, DMSO) δ 173.5, 168.6, 37.2; **ESI-LC-MS** m/z 117 [M + H]⁺ (Calculated. For C₃H₃NO₂S).

Step 2: Synthesis of 3-(4-nitrobenzyl) thiazolidine-2,4-dione (4)

With the aid of thiazolidine-2,4-dione **3** (1 mmol) was continuously stirred to which 5 mL dry DMF was added. To the above solution 1 mmol of 4-nitro benzyl bromide was added in parts while continuous stirring. The solution was stirred for another 10-15 min. Further the 1.2 mmol of potassium carbonate was added as base in the reaction. Stirring continued till all the starting materials were consumed. The reaction was monitored by using TLC (MP: n-hexane: ethyl acetate 7:3). On completion, the reaction mixture was transferred to ice cold water dropwise with continuous stirring while the product precipitated out. The product was washed with excess amount of cold water to remove traces of alkali. The obtained fluffy product was then recrystallized using hot ethanol. (Singh et al., 2024)

4: 3-(4-nitrobenzyl) thiazolidine-2,4-dione: Buff Colour; ¹**H NMR (500 MHz, DMSO)** δ 8.24 (d, J = 8.5 Hz, 2H), 7.60 (d, J = 8.6 Hz, 2H), 5.00 (s, 2H), 4.1 (s, 2H); **13C NMR (126 MHz, DMSO)** δ 168.5, 165.6, 145.9, 142.6, 127.8, 123.7, 46.9, 37.2; **ESI-LC-MS** m/z 253 [M + H]⁺ (Calcd. For C₁₀H₈N₂O₄S).

Step 3: Synthesis of (Z)-5-benzylidene-3-(4-nitrobenzyl) thiazolidine-2,4-dione (5-18)

The final product (**5-18**) was prepared by using a well-known Knoevenagel condensation. One mmol of 3-(4-nitrobenzyl) thiazolidine-2,4-dione **4** was suspended in dry ethanol (10 mL) along with 1 mmol of respective aldehydes (5-18). To this solution catalytic amount of piperidine and acetic acid were added, and reaction mixture was refluxed at 75 °C for 5-7hrs. The completion of reaction was monitored by using TLC (MP: n-hexane: ethyl acetate 7:3). The final product was obtained by evaporating ethanol and suspending the product in cold water. The obtained product was washed with cold water to remove the excessive amount of catalyst present. The yellow to brown colored products were recrystallized using hot ethanol. (Singh *et al.*, 2024)

The characterization of synthesized compounds was performed by ¹H NMR, ¹³C NMR, Mass Spectrometry.



Characterization of synthesized compounds 5-18

Compound 5: (Z)-5-((2-hydroxynaphthalen-1-yl) methylene)-3-(4-nitrobenzyl) thiazolidine-2,4-dione 1 **H NMR (500 MHz, DMSO)** δ 9.21 (s, 1H), 8.37 (s, 1H), 8.24 (d, J = 8.5 Hz, 2H), 8.18 (d, J = 8.7 Hz, 2H), 7.87 (dd, J = 23.1, 8.5 Hz, 1H), 7.78 (d, J = 8.5 Hz, 1H), 7.62 (d, J = 8.9 Hz, 1H), 7.52 (dd, J = 17.6, 7.9 Hz, 1H), 7.13 (, 1H), 4.98 (s, 2H). **13C NMR (126 MHz, DMSO)** δ 168.5, 165.6, 157.2, 149.6, 146.2, 143.3, 132.7, 129.9, 128.8, 127.9, 123.9, 123.5, 123.4, 122.5, 120.3, 118.4, 44.4, 40.1, 40.0, 39.9, 39.9, 39.8, 39.7, 39.6, 39.5, 39.4, 39.2, 39.0; **ESI-HR-MS** m/z 406.8040 [M + 1H]⁺ (Calcd. For C₂₁H₁₄N₂O₅S).

Compound 6: (Z)-3-((3-(4-nitrobenzyl)-2,4-dioxothiazolidin-5-ylidene) methyl) benzaldehyde **H NMR (500 MHz, CDCl₃)** δ 10.07 (s, 1H), 8.19 (dd, J = 20.1, 8.6 Hz, 1H), 7.98 (d, J = 9.3 Hz, 1H), 7.92 (s, 1H), 7.75 (d, J = 7.5 Hz, 1H), 7.60 (d, J = 8.6 Hz, 2H), 7.56 (d, J = 8.5 Hz, 2H), 7.47 (s, 1H), 5.00 (s, 2H). **CDCl₃**) δ 191.2, 167.1, 165.7, 148.1, 141.8, 137.3, 135.4, 134.8, 134.3, 130.5, 129.9, 128.2, 124.2, 123.9, 122.9, 77.4, 77.4, 77.2, 76.9, 45.2. **ESI-HR-MS** m/z 369.1166 [M + 1H]⁺ (Calcd. For $C_{18}H_{12}N_2O_5S$).

Compound 7: (Z)-3-(4-nitrobenzyl)-5-(4-(pyridin-2-yl) benzylidene) thiazolidine-2,4-dione **1H NMR (500 MHz, CDCl₃)** δ 8.72 (d, J = 4.8 Hz, 1H), 8.21 (d, J = 8.7 Hz, 2H), 8.13 (d, J = 8.3 Hz, 2H), 7.98 (s, 1H), 7.79 (d, J = 4.6 Hz, 2H), 7.61 (dd, J = 8.5, 4.1 Hz, 4H), 7.29 (dd, J = 11.1, 2.4 Hz, 1H), 5.00 (s, 2H). **13C NMR (126 MHz, CDCl₃)** δ 167.8, 166.0, 155.9, 150.1, 148.0, 142.1, 141.6, 137.1, 134.5, 133.5, 130.9, 129.8, 127.8, 124.2, 123.1, 121.3, 120.9, 77.4, 77.2, 76.9, 44.5. **ESI-HR-MS** m/z 418.0854 [M + 1H]⁺ (Calcd. For C₂₂H₁₅N₃O₄S).

Compound 8: (Z)-5-(3-(4-nitrobenzyl)-2,4-dioxothiazolidin-5-ylidene) pentanal ¹**H NMR (500 MHz, DMSO)** δ 9.50 (t, 1H), 8.20 (d, J = 8.5 Hz, 2H), 7.51 (d, J = 8.2 Hz, 2H), 6.87 (t, J = 6.2 Hz, 1H), 4.36 (s, 2H), 3.13 (dt, J = 176.5, 5.7 Hz, 2H), 1.68 – 1.18 (m, 4H). ¹³**C NMR (126 MHz, DMSO)** δ 208.7, 172.6, 158.1, 149.3, 146.3, 142.6, 127.9, 123.5, 44.4, 42.6, 40.1, 40.0, 39.9, 39.9, 39.8, 39.7, 39.6, 39.5, 39.4, 39.2, 39.0, 25.4, 24.2. **ESI-HR-MS** m/z 334.7746 [M + 1H]⁺ (Calcd. For C₁₅H₁₄N₂O₅S).

Compound 9: (Z)-5-(3,5-dichloro-2-hydroxybenzylidene)-3-(4-nitrobenzyl) thiazolidine-2,4-dione **H NMR (500 MHz, CDCl₃)** δ 9.86 (s, 1H), 8.23 – 8.17 (m, 3H), 7.59 (d, J = 8.8 Hz, 2H), 7.38 (s, 1H), 7.25 (s, 1H), 4.97 (s, 2H). ¹³**C NMR (126 MHz, CDCl₃)** δ 167.7, 166.0,155.3, 148.0, 142.1, 141.6, 131.2, 129.8, 129.6, 128.2, 127.7, 124.2, 123.2, 119.3, 77.4, 77.4, 77.2, 76.9, 44.5. **ESI-HR-MS** m/z 425.1168 [M + 1H]⁺ (Calcd. For C₁₇H₁₀N₂O₅SCl₂).

Compound 10: (Z)-5-(2-hydroxybenzylidene)-3-(4-nitrobenzyl) thiazolidine-2,4-dione ¹H NMR (500 MHz, DMSO) δ 9.21 (s, 1H), 8.37 (s, 1H), 8.24 (d, J = 8.5 Hz, 2H), 8.18 (d, J = 8.7 Hz, 2H), 8.03 (d, J = 8.2 Hz, 1H), 7.86 (dd, J = 23.1, 8.5 Hz, 1H), 7.77 (d, J = 8.5 Hz, 1H), 7.51 (dd, J = 17.6, 7.9 Hz, 1H), 4.98 (s, 2H). ¹³C NMR (126 MHz, DMSO) δ 168.8, 165.6, 157.2, 149.6, 146.2, 143.3, 132.7, 128.8, 127.9, 123.9, 123.5, 123.4, 120.3, 118.4, 44.4, 40.1, 40.0, 39.9, 39.9, 39.8, 39.7, 39.6, 39.5, 39.4, 39.2, 39.0. **ESI-HR-MS** m/z 353.8800 [M + 1H]⁺ (Calcd. For $C_{17}H_{12}N_2O_5S$).

Compound 11: (Z)-4-((3-(4-nitrobenzyl)-2,4-dioxothiazolidin-5-ylidene) methyl) benzaldehyde ¹H NMR (500 MHz, CDCl₃) δ 10.07 (s, 1H), 8.21 (d, J = 8.6 Hz, 2H), 7.92 (s, 1H), 7.60 (d, J = 8.6 Hz, 3H), 7.56 (d, J = 8.5 Hz, 1H), 7.46 (d, J = 6.7 Hz, 2H), 5.00 (s, 2H). ¹³C NMR (126 MHz, CDCl₃) δ 191.2, 167.1, 165.7, 148.1, 141.8, 137.3, 135.4, 134.8, 129.9, 128.2, 123.9, 122.9, 77.4, 77.4, 77.2, 76.9, 44.7. **ESI-HR-MS** m/z 369.0088 [M + 1H]⁺ (Calcd. For $C_{18}H_{12}N_2O_5S$).

Compound 12: (Z)-3-(4-nitrobenzyl)-5-(pyridin-2-ylmethylene) thiazolidine-2,4-dione **1H NMR (500 MHz, CDCl₃)** δ 8.72 (d, J = 4.8 Hz, 1H), 8.21 (d, J = 8.7 Hz, 2H), 8.13 (d, J = 8.3 Hz, 2H), 7.98 (s, 1H), 7.79 (d, J = 1.5 Hz, 1H), 7.61 (dd, J = 8.5, 4.1 Hz, 2H), 5.00 (s, 2H). **13C NMR (126 MHz, CDCl₃)** δ 168.2, 165.8, 157.5, 147.9, 147.8, 142.2, 139.4, 135.2, 127.7, 124.1, 123.9, 122.3, 119.6, 77.4, 77.4, 77.2, 76.9, 44.4. **ESI-HR-MS** m/z 342.0853 [M + 1H]⁺ (Calcd. For C₁₆H₁₁N₃O₄S).

Compound 13: (Z)-5-(2-hydroxy-3-methoxybenzylidene)-3-(4-nitrobenzyl) thiazolidine-2,4-dione ¹H NMR (500 MHz, CDCl₃) δ 10.07 (s, 1H), 8.21 (d, J = 8.6 Hz, 2H), 7.98 (d, J = 9.3 Hz, 1H), 7.92 (s, 1H), 7.60 (d, J = 8.6 Hz, 2H), 7.56 (d, J = 8.5 Hz, 1H), 7.46 (d, J = 8.6 Hz, 1H), 5.00 (s, 2H), 3.37 (s, 3H). ¹³C NMR (126 MHz, CDCl₃) δ 168.2, 165.8, 157.5, 147.9, 147.2, 142.1, 139.4, 127.7, 124.1, 123.9, 122.3, 119.6, 117.1, 111.9, 77.4, 77.4, 77.2, 76.9, 56.2, 44.4.

ESI-HR-MS m/z 387.0739 $[M + 1H]^+$ (Calcd. For $C_{18}H_{14}N_2O_6S$).

Compound 14: (Z)-5-(3,4-dichlorobenzylidene)-3-(4-nitrobenzyl) thiazolidine-2,4-dione



¹H NMR (500 MHz, CDCl₃) δ 8.23 – 8.17 (m, 3H), 7.59 (d, J = 8.8 Hz, 2H), 7.46 (d, J = 8.0 Hz, 1H), 7.37 (d, J = 2.4 Hz, 1H), 7.25 (s, 1H), 4.97 (s, 2H). ¹³C NMR (126 MHz, CDCl₃) δ 167.7, 166.0, 148.0, 142.1, 141.0, 131.2, 129.8, 129.6, 128.2, 127.7, 124.2, 123.2, 117.0, 77.4, 77.4, 77.2, 76.9, 44.5. ESI-HR-MS m/z 409.2040 [M + 1H]⁺ (Calcd. For C₁₇H₁₀N₂O₄SCl₂).

Compound 15: (Z)-3-(4-nitrobenzyl)-5-(2-oxo-2-phenylethylidene) thiazolidine-2,4-dione ¹**H NMR (500 MHz, CDCl₃)** δ 8.72 (d, J = 4.8 Hz, 1H), 8.21 (d, J = 8.7 Hz, 2H), 8.13 (d, J = 8.3 Hz, 2H), 7.98 (s, 1H), 7.79 (d, J = 1.5 Hz, 2H), 7.61 (dd, J = 8.5, 4.1 Hz, 2H), 5.00 (s, 2H). ¹³**C NMR (126 MHz, CDCl₃)** δ 190.7, 168.2, 165.8, 147.9, 142.1, 139.4, 135.2, 133.1, 131.3, 129.8, 127.7, 124.1, 119.6, 77.4, 77.2, 76.9, 44.4. **ESI-HR-MS** m/z 369.1166 [M + 1H]⁺ (Calcd. For $C_{18}H_{12}N_2O_5S$).

Compound 16: (Z)-5-(3-methylbenzylidene)-3-(4-nitrobenzyl) thiazolidine-2,4-dione **1H NMR (500 MHz, CDCl₃)** δ 8.21 (d, J = 8.7 Hz, 2H), 8.15 (s, 1H), 7.61 (d, J = 8.6 Hz, 2H), 7.42 (dd, J = 16.1, 7.4 Hz, 1H), 7.34 (s, 1H), 7.29 (d, J = 6.2 Hz, 2H), 4.98 (s, 2H), 2.44 (s, 3H). **13C NMR (126 MHz, CDCl₃)** δ 168.2, 165.8, 147.9, 142.2, 141.9, 139.4, 133.1, 130.9, 130.2, 129.8,127.7, 126.7, 124.1, 122.3, 77.4, 77.2, 76.9, 44.4, 20.0. **ESI-HR-MS** m/z 354.8343 [M + 1H]⁺ (Calcd. For C₁₈H₁₄N₂O₄S).

Compound 17: (Z)-5-(2,6-difluorobenzylidene)-3-(4-nitrobenzyl) thiazolidine-2,4-dione ¹H NMR (500 MHz, CDCl₃) δ 8.21 (d, J = 8.6 Hz, 2H), 7.92 (s, 1H), 7.60 (d, J = 8.7 Hz, 2H), 7.56 (d, J = 8.5 Hz, 1H), 7.46 (d, J = 8.9 Hz, 2H), 5.00 (s, 2H). ¹³C NMR (126 MHz, CDCl₃) δ 167.8, 166.0, 155.9, 148.0, 142.1, 141.6, 129.8, 127.8, 124.2, 120.9, 112.6, 111.0, 77.4, 77.2, 76.9, 44.5. **ESI-HR-MS** m/z 377.2134 [M + 1H]⁺ (Calcd. For C₁₇H₁₀N₂O₄SF₂).

Compound 18: (Z)-5-(5-chloro-2-hydroxybenzylidene)-3-(4-nitrobenzyl) thiazolidine-2,4-dione ${}^{1}\mathbf{H}$ **NMR** (**500 MHz, CDCl₃**) δ 10.28 (s, 1H), 8.24 – 8.19 (m, 3H), 7.61 (d, J = 8.8 Hz, 2H), 7.48 (d, J = 8.3 Hz, 1H), 7.39 (d, J = 2.4 Hz, 1H), 7.28 (s, 1H), 4.99 (s, 2H). ${}^{13}\mathbf{C}$ **NMR** (**126 MHz, CDCl₃**) δ 167.0, 165.6, 154.5, 147.9, 142.8, 141.7, 131.5, 129.8, 128.1, 124.1, 123.8, 122.8, 118.9, 117.2, 77.3, 77.2, 77.0, 76.8, 45.1. **ESI-HR-MS** m/z 391.0796 [M + 1H]⁺ (Calcd. For $\mathbf{C}_{17}\mathbf{H}_{11}\mathbf{N}_{2}\mathbf{O}_{5}\mathbf{SCl}$).

2.3 In-vitro enzyme inhibition assay:

Calbiochem PTP1B Colorimetric Assay Kit (Calbiochem PTP1B Assay Kit, Colorimetric, User Protocol, 2008, Catalogue No: 539736) was used for the assessment of inhibitory potential of the final compounds 5-18. The E.coli expressed human recombinant PTP1B (residues 1-322; MW 37,400) was provided in the kit. The basic aim was quantify the release of free phosphate produced by hydrolysis of IR5 phosphopeptide substrate by PTP1B enzyme. The absorbance of the same were detected at wavelength of 620 nm. Manufacturer's protocols were followed to carry out the experimentation under suitable conditions. Suramin were consider as reference standard whereas working test solution of compounds 5-18 were prepared using DMSO as solvent. To evaluate the inhibition activity of test compounds on PTP1B, a reaction mixture was prepared by combining 35 μL of assay buffer (containing 300 mM NaCl, 100 mM MES, 2 mM DTT, 2 mM EDTA, 0.1% NP-40, pH 7.2) pre-warmed to 30°C. This was followed by the addition of 10 μl of a solubilizing solution, which could be either the control or the inhibitor solution at five different concentrations. Next, 5 µL of the diluted PTP1B enzyme was included, sourced from human recombinant PTP1B (residues 1-322; MW 37400), expressed in E. coli at a concentration of 100 ng/μL, in a buffer containing 50 mM HEPES, 1 mM EDTA, 1 mM DTT, 10% v/v glycerol, and 0.05% NP-40, pH 7.2. The reaction was initiated by adding 50 µl of the warmed PTP1B substrate (IR5, which consists of amino acids 1142-1153, pY1146, MW 1703 kDa). The reaction was initiated by adding 50 µL of the warmed PTP1B substrate (IR5, which consists of amino acids 1142-1153, pY1146, MW 1703 kDa). The Incubation time for mixture was 30 minutes at 30°C and reaction termination was performed by addition of phosphate detection reagents (red Reagent). The mixing of mixture was then performed and allowed to stand for about 30 minutes to develop colour. The absorbance was measured at 620 nm microplate reader. Control experiments were carried out without inhibitor and blanks were run without PTP1B enzyme. All the assays were performed in triplicates. IC₅₀ values were calculated, along with the 95% confidence limits, with GraphPad Prism Software (version 5.0), using plots of inhibition percentages versus the logarithm of the inhibitor concentration. Additionally, All the compounds 5-18 were subjected to UV visible spectral analysis and found that no compound have absorbed in the wavelength of 620nm. (Patel et al., 2020)

RESULTS AND DISCUSSION:

3.1 In-silico drug design

FBDD approach was used to find compounds that can inhibit PTP1B enzyme. The protein PDB (id:1T49) was downloaded from RCBS.org. PDB 1T49 contain inhibitor of enzyme that is present in the allosteric site of protein. Due to this PDB id 1T49 was selected for designing of new inhibitors of Allosteric site of PTP1B enzyme. The allosteric site was found surrounded by α -3 helix, α -6 helix and α -7 helix.

In FBDD, 253 fragments, generated from 19 inhibitors of PTP1B were prepared and their docking (SP mode) of same was performed. The docking score of all the diversified fragments were observed in the range of -7.476 to -3.20. Ninety seven fragments were identified having docking scores less than -6.0 while 428 molecules were designed by joining of 97 fragments as per their binding overlaps. Molecular docking of these molecules revealed their good affinity toward enzyme. The docking score of these molecules ranged from -7.9 to -2.8. Based on docking top 10 compounds were selected for further analysis. Of these compounds, Compound **a** (Fig 2) had given docking score of -7.9 and was also present in the desired pocket and was bound to amino acid participated in enzyme inhibition. The interaction of Compound a with allosteric site is given below along with site map (Fig 2). The synthetic accessibility (Swissadme) value of this compound was found to be 3.30 Swiss ADME server (Daina *et al.*, 2017). This compound **a** (Fig No: 2) was considered as hit for the PTP1B enzyme.

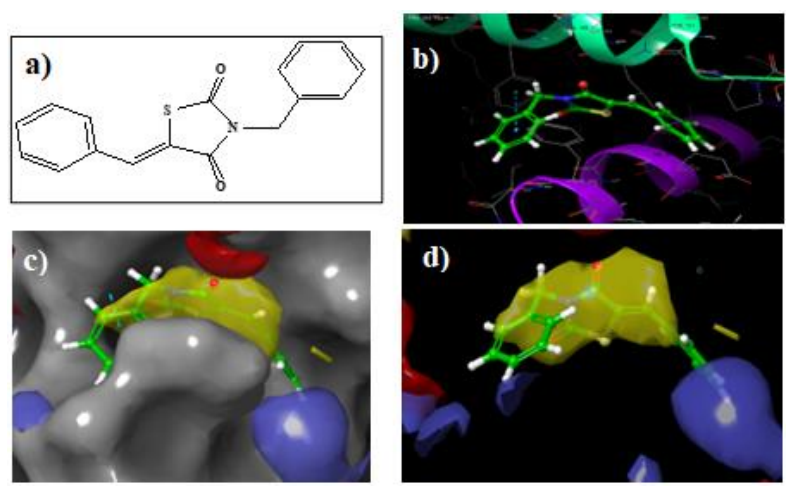


Fig 2: a) Structure of compound a; b) Protein-ligand interaction; c) Compounds in the active site of enzyme; d) Compounds and the site map of the enzyme

The 48 derivatives based on reaction-based enumeration were designed hit to lead generation. In this, the benzyl substitution on N-3 was substituted with nitro group whereas the benzylidene substitution on 5^{th} position wewas taken from the substituted benzaldehyde. Molecular docking (SP MODE) of these molecules was performed as per protocol. Top 14 derivatives depicted docking score \geq 8.0 and were selected based on their drug likeliness and pharmacokinetic properties (Table). The compound 5 had shown lowest docking score of -9.22 with RMSD value 1.088 (with Co-crystal ligand). Docking score of compounds 5-18 are depicted in Table 1. The docking analysis of these showed important interactions with various amino acid important for enzyme inhibition. The compound 5 had good interaction which include π - π stacking of naphthalene ring in the structure with PHE 196 and PHE 280 with less than 5Å distance and the nitro substitution on N-3 benzyl have formed salt bridge with LYS279 and GLU276 with very less distances 4.28 and 4.96Å, respectively (Fig: 3). Important interaction shown by other derivatives included π - π stacking (distance ranges <5.0), hydrogen bonding (<2.5Å), salt bridge (<5Å), halogen bonds (<3.2Å) and π -cation interaction (<4Å).

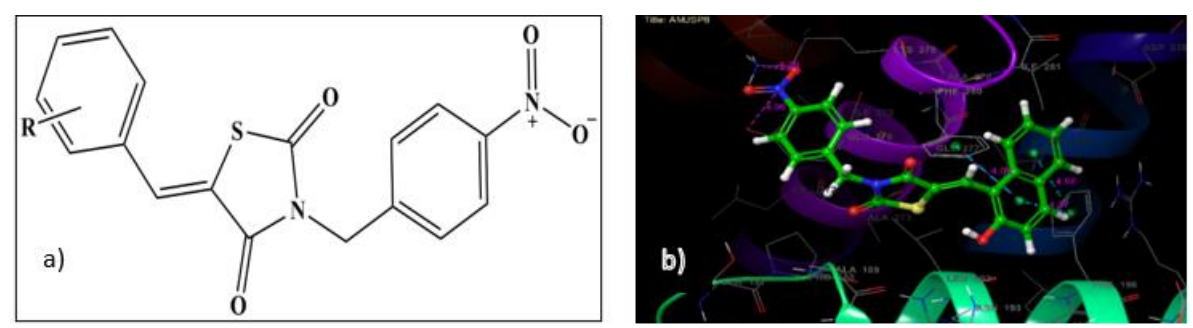


Fig 3: a) Proposed Compound b) Interaction of compound 5 with Allosteric site of PTP1B enzyme

Pose analysis & binding modes of designed compounds (5-18):

The visual examination of above docked compounds was performed (Fig.1-b). This examination revealed that all the designed compounds occupied the allosteric site of the PTP1B enzyme. The interactions that contributed for the stabilization of ligand-protein complex were majorly salt bridge, hydrogen bonding and hydrophobic interactions along with π -cation, π - π stacking and halogen bonds.



All the compounds, except compound **05**, **12** and **17** showed one-or more hydrogen bond interaction. The amino acid involved in the interaction is mainly SER187, ASN 193 and GLU276. The H-bond interaction of residue ASN193 was observed for all the compounds except compounds **5**, **6**, **12** and **17**. Similarly SER187 depicted H-bond interaction with compound **6**, GLU276 residue with compound **14**.

In addition to this, compounds **5**, **6**, **10**, **15** and **16** formed salt bridges as well. The amino acids formed salt bridge with the ligand molecules were ARG199, LYS279, GLU276. The residue ARG 199 have formed salt bridges with compounds **6**, **10**, **15** and **16** whereas LYS279 and GLU276 formed salt bridge with compound **5**.

In docking analysis, hydrophobic interaction also plays an important role binding of molecules. These interactions include π - π stacking, π -cation and halogen bond interactions. The π - π Stacking was mainly observed with amino acid PHE196 and PHE280. The amino acid residue PHE196 showed π - π stacking with all the compounds (**5-18**) and is one of the important interactions as the inhibition is considered. The residue PHE280 exhibited π - π Stacking with compounds **5, 11, 12** and **13**. Interplanar distance of all the hydrophobic interaction was found to be <5.0Å. Two compounds **7** and **17** showed π -cation interaction with amino acid ARG199 with interplanar distance 5.33 and 4.29 Å respectively. Halogen bond interaction was shown by compounds **13** and **18** with SER187 having interplanar distance 3.16 and 3.0 Å respectively.

3.2 Chemistry:

Fourteen novel thiazolidin-2,4-dione derivatives (5-18) designed in this study were synthesized as per synthetic route in **scheme 1** with standard reaction conditions. The first intermediate **3** was a condensation product of **1** and **2**. Further this compound **3** was reacted with 4-nitro benzyl bromide to yield compound **4**. The final step of reaction followed the Knoevenagel condensation where final compounds (5-18) were product of condensation of **4** and respective aldehydes. The physicochemical properties and spectral characterization were in good agreement with the structural data and are given in material and method section.

The physicochemical properties of the compounds (5-18) and thier docking scores are given in Table:1

Table 1: Physicochemical Characterization of Compounds 5-18

Sr. No	Compd	R	Docking score	Melting point (°C)	Yield (% w/w)
1.	5	W	-9.228	208-211	86.25
2.	6	3-CHO	-8.772	190-195	54.79
3.	7	4-(pyridine-2-yl)	-8.697	204-208	81.81
4.	8	W	-8.635	165-170	90.90
5.	9	3,5-Cl, 2-OH	-ОН -8.626		95.23
6.	10	2-OH	-8.621	160-166	81.56
7.	11	4-CHO	-8.555	284-283	95.89
8.	12	W	-8.555	168-172	85.18
9.	13	2-OH,3-OCH ₃	-8.514	177-181	68.62
10.	14	3,4- Cl	-8.42	165-168	53.66
11.	15	W	-8.386	155-158	54.79
12.	16	3-CH ₃	-8.383	162-164	85.71
13.	17	2,6-di F	-8.337	100-110	46.97
14.	18	5-Cl,2-OH	-8.273	72-76	84.41

W= as per the structure given in the scheme 1

3.3 In-silico drug-likeness and pharmacokinetic property prediction:

All the synthesized compounds were subjected for Lipinski's rule's screening to identify drug-likeness (Table 2). For this purpose, pkCSM server was used. The lipophilicity (LogP) predicted that the compounds **5-18** were in range of 3.04 to 4.98 which is <5, so accepted for drug design. The molecular weight of all the compounds were < 500 which is essential for biological membranes penetration. The surface area (SA) all the compounds was in the range of $136.041-175.753\text{Å}^2$, and the values were within the limit. All the above-mentioned values indicated the good bioavailability of all the compounds. The compounds **5-18** also followed the Lipinski's rule of five in accordance with no of H-bond acceptors (HBA, ≤ 10) and H-bond donors (HBD, ≤ 5). Thus, oral activity of all the compounds was predicted based on these values.

Table 2: Drug Likeliness in-silico prediction (Compound 5-18)

				1			
Compound	Molecular Weight (Dalton)	LogP	Rotatable bonds	H-bond acceptors	H-bond donors	Lipinski violation	Surface Area (A ²)

5	406.419	4.6901	4	6	1	0	168.953
6	368.37	3.6438	5	6	0	0	152.003
7	417.446	4.8933	5	6	0	0	175.753
8	334.353	3.0433	7	6	0	0	136.041
9	425.249	4.8437	4	6	1	0	166.878
10	356.359	3.5369	4	6	1	0	146.271
11	368.37	3.6438	5	6	0	0	152.003
12	341.348	3.2263	4	6	0	0	140.696
13	386.385	3.5455	5	7	1	0	157.749
14	409.25	5.1381	4	5	0	0	162.083
15	368.37	3.557	5	6	0	0	152.003
16	354.387	4.13972	4	5	0	0	147.842
17	376.34	4.1095	4	5	0	0	149.808
18	390.804	4.1903	4	6	1	0	156.574

Additionally, pkCSM server was used for ADMET analysis (Table 3). The water solubility of all the compounds was from –6.162 log mol L⁻¹ (compound 9) to -4.621 to log mol L⁻¹ (compound 8). The Caco-2 permeability of all the compounds was high (permeation > 0.80), except for compounds **7, 14, 16** and **17** (permeation = 0.502, 0.501, 0.465, and 0.698) which was moderate, and compound **13** (permeation = 0.099) with poor permeability. Intestinal membrane permeation was found to be good as the intestinal absorption (IA) of all the compounds was greater than 88%. Further, the skin permeability of all the compounds **5-18** was poor (permeation < -2.5). Additionally, P-glycoprotein I inhibition was predicted by all compounds, except compound **8,** had shown no inhibition towards P-glycoprotein I, whereas compounds 8, 10-12, 15 and 17 have no inhibition of P-glycoprotein II and rest compounds showed inhibition of P-glycoprotein II. Further, BBB permeability of all compounds was poor whereas CNS permeability was moderate. Except compound **8, 10** and **16,** all other compounds showed CYP3A4 inhibition property, whereas all the compounds possessed inhibitory property against CYP2C9 enzyme, which indicated the reduction of xenobiotic agent metabolism. Compounds **5-18** exhibited total clearance values between -0.007 and 0.259 (log mL min⁻¹ kg⁻¹) and were not found to be OCT2 substrates, suggesting the likelihood of adverse interactions and detrimental effects on renal clearance.

Table 3: ADME in-silico prediction of Synthesized Compound 5-18

Comp	Absorption						Distribution				Metabolis m		Excretion	
d	WS	СР	IA	SP	PI- 1	PI2	VD	FU	BBB	CNS	CI- 1	CI- 2	TC	RS
5	5.70 5	1.09	96.05 8	2.73	Yes	Yes	- 0.14 5	0	- 0.40 4	1.92 8	Yes	Yes	0.07	No
6	5.69 7	1.18 1	95.87 1	2.72 9	Yes	Yes	-0.29	0	- 0.54 6	- 2.21 4	Yes	Yes	0.06 8	No
7	-5.71	0.50	100	- 2.74 8	Yes	Yes	- 0.17 9	0	- 0.56 6	- 1.84 5	Yes	Yes	0.11 5	No
8	- 4.62 8	0.99	89.84 7	2.89 3	No	No	- 0.34 4	0.05 5	- 0.73 4	- 2.54 8	No	Yes	0.18 8	No
9	6.16 2	0.84 5	91.16 5	2.72 9	Yes	Yes	- 0.23 4	0	- 0.84 3	- 1.95 6	Yes	Yes	0.10	No
10	5.12 8	1.02	88.87 1	- 2.72 4	Yes	No	- 0.18 4	0	- 0.48 6	2.18 7	No	Yes	0.12	No
11	5.50 2	0.97 9	92.91	- 2.82 9	Yes	No	- 0.28 8	0	- 0.58 4	2.19 8	Yes	Yes	0.11 6	No



12	- 4.72 3	0.97 4	98.52 3	- 2.96 9	Yes	No	- 0.41 6	0.06	-0.79	2.27 1	Yes	Yes	0.11	No
13	- 4.80 9	0.09 9	86.08 9	2.76 5	Yes	Yes	- 0.31 9	0	- 0.57 1	2.32 6	Yes	Yes	0.25 9	No
14	- 6.59 7	0.50 1	89.06 8	2.79 4	Yes	Yes	- 0.09 6	0	- 0.70 9	- 1.74 4	Yes	Yes	0.11 8	No
15	-5.34	1.12 5	88.51 8	2.82 8	Yes	No	- 0.37 1	0	- 0.62 1	2.21 3	Yes	Yes	0.21 7	No
16	5.62 4	0.46 5	89.02 7	2.68 3	Yes	Yes	0.13 4	0	- 0.30 9	- 1.90 7	No	Yes	0.07	No
17	5.90 6	0.69 8	90.29	- 2.81 9	Yes	No	- 0.41 9	0	- 0.76 1	- 2.05 9	Yes	Yes	0.00 6	No
18	5.66 8	0.85 6	89.98 9	2.72 7	Yes	Yes	-0.22	0	- 0.69 1	2.07 1	Yes	Yes	- 0.00 7	No

WS: Water solubility; CP: Caco-2 permeability; IA: Intestinal absorption; SP: Skin permeability; PI: P-glycoprotein; VD: Human volume of distribution; FU: Fraction unbound; BBB: BBB permeability; CNS: CNS permeability; CI-1: CYP3A4 Inhibitor; CI-2: CYP2C9 inhibitor; TC: Total Clearance; RS: Renal Clearance.

With reference to toxicity (Table No: 4), all the compounds **5-18** have predicted to show AMES toxicity except **17** and hence can be mutagenic in nature. The Maximum recommended tolerated dose (human) for all compounds were predicted in the range of -0.524 log mg/kg/day (compound **5**) to 0.171 log mg/kg/day (compound **6**), indicating Low MRTD for all the compounds. All the compounds **5-18** were predicted for negative response as hERG I inhibitors; whereas compounds **6**, **7**, **9**, **12**, **13**, and **16** were predicted to be hERG II inhibitors indicating their potential long QT syndrome development which may further lead to ventricular arrhythmia. As per the prediction, the LD₅₀ value of Oral rat acute toxicity (ORAT) lie in the range of 2.378 mol/kg (compound **15**) to 3.428 mol/kg (compound **07**). Moreover, the range of oral rat chronic toxicity (ORCT) models predicted the LOAEL values was found to be 1.078 log mg/kg_bw/day (compound **9**) to 2.41 log mg/kg_bw/day (compound **13**).

All the compounds except **6-11, 13**, and **15** were not predicted to impair liver function or exhibit skin sensitivity, yet all demonstrated toxicity to T. pyriformis and minnows.

Table 4: Toxicity *in-silico* prediction (Compound 5-18)

Compd	AT	MRTD	hERG	hERG	ORat	ORCT	HT	SS	TPT	MT
_			I	II						
5	Yes	-0.524	No	No	2.726	1.372	No	No	0.64	0.197
6	Yes	0.171	No	Yes	2.517	1.677	Yes	No	0.536	0.148
7	Yes	-0.513	No	Yes	3.428	1.566	Yes	No	0.408	-0.242
8	Yes	-0.518	No	No	2.615	1.557	Yes	No	0.689	0.511
9	Yes	-0.084	No	Yes	2.517	1.078	Yes	No	0.326	0.261
10	Yes	-0.121	No	No	2.458	1.671	Yes	No	0.977	-0.21
11	Yes	-0.069	No	No	2.817	1.45	Yes	No	0.979	0.169
12	Yes	-0.12	No	Yes	2.522	2.251	No	No	0.796	-0.005
13	Yes	-0.163	No	Yes	2.647	2.41	Yes	No	0.439	-0.052
14	Yes	-0.077	No	No	2.828	1.626	No	No	1.088	-1.128
15	Yes	0.159	No	No	2.378	1.946	Yes	No	0.611	0.098
16	Yes	-0.458	No	Yes	2.61	1.667	No	No	0.691	0.958
17	No	-0.104	No	No	2.509	1.424	No	No	1.193	-0.219
18	Yes	-0.139	No	No	2.233	2.342	No	No	0.529	-0.608



AT: AMES Toxicity; MRTD: Maximum Recommended Tolerated Dose, hERG inhibition, ORat: oral rat toxicity, ORCT: oral chronic toxicity, HT: hepatotoxicity, SS: skin sensitization, TPT: total polar surface area, MT metabolic transformation.

3.4 In-vitro PTP1B enzyme inhibition assay:

All the shortlisted and synthesized derivatives were subjected for *in-vitro* assay to identify the potential of compounds **5-18** as PTP1B inhibitor. The *in-vitro* Colorimetric assay was performed using Calbiochem PTP1B assay kit and suramin as reference inhibitor. The inhibitory activities were studied by assessing how each compound affected the production of free phosphate from the IR5 phosphopeptide substrate. The results of inhibition assays are expressed as IC₅₀ values and are compiled in Table 5.

Table 5: In-vitro Analysis of synthesized compounds 5-18

Table 5: In-vitro Analysis of synthesized compounds 5-18									
Compound	IC50 µM (Mean± SEM)	Docking Score							
Suramin	10	-							
Sodium Vanadate	14.68	-							
5	27.32 ± 0.80	-9.228							
6	34.29 ± 0.32	-8.772							
7	4.14 ± 0.99	-8.697							
8	63.58 ± 0.70	-8.635							
9	15.20 ± 0.58	-8.626							
10	105.10 ± 0.18	-8.621							
11	29.31 ± 0.24	-8.555							
12	5.25 ± 0.28	-8.555							
13	26.35 ± 0.62	-8.514							
14	96.57 ± 1.03	-8.42							
15	49.44 ± 0.35	-8.386							
16	46.50 ± 0.46	-8.383							
17	36.11 ± 0.55	-8.337							
18	38.84 ± 0.20	-8.273							

The IC₅₀ values of the synthesized compounds (**5-18**) ranged from 4.14±1.01 (compound **7**) **to** 105.10±0.30 (compound **10**). Suramin and sodium vandate was used as standard inhibitors of enzymes. Two compound **7** and 12 depicted lesser IC₅₀ values as compared to both the standards whereas compound 9 gave comparable IC₅₀ with respect to standards. Compounds 7, 12, 09, 13, 05 and 11 showed good to moderate inhibitory activity for the enzyme. The results pinpoint the importance of various substitution at 5th position of TZD ring. Further, it was observed that the ring substitution at para position of benzylidene ring may help to increase the activity. The modification in steric and electronic parameters of these compounds was tested by incorporation of various substitution such as Cl, F, -OH, -CHO, -CH₃ etc. at various positions of benzylidene ring. Beside from pyridine substitution at para position of benzylidene ring, only pyridine ring instead of phenyl ring (compounds **12**) also have given good IC₅₀ value, followed by compound **9** which have 3,5-dichlro along with 2 hydroxy group presents on the benzylidene ring. Interestingly the compounds having electron donating group specifically -OH showed inhibition of enzyme to better extent along with electronegative atoms present on the benzylidene ring, but when only -OH was considered at ortho position, the compounds showed minimal activity. The activity of compounds has been very less when benzylidene nucleus if replaced by aliphatic chain as in compound **8.** But replacement of benzylidene nucleus with other heteroaromatic (compound **12**) nucleus showed inhibition at lower concentration.

CONCLUSION:

In present study, a series of thiazolidione-2,4-dione derivatives (5-18) were examined for their potential as PTP1B allosteric inhibitors which aim at collecting the information about their further application as potential antidiabetic and anti-obesity agents. Surprisingly all the compounds showed inhibitory activity against enzyme PTP1B. Compound 7 exhibited better inhibitory potential with IC_{50} value of 4.14 ± 1.71 followed by

compound **12** (5.25±0.48 µM) and compound **9** (15.20±1.01 µM). but the activity was drastically reduced when benzylidene was replaced by alkyl side chain. This study indicated that benzylidene or any aromatic nucleus at 5th position of TZD is essential for acidity. H bond acceptor group on benzylidene have shown to elevate the activity. The molecular docking of these agents has also shown the area for substitution of benzylidene ring with different H bond acceptor & donors. The compound **7** were found to interact with

enzyme through H-bonding, π - π Stacking and π -cation interactions. The distance of H bond formed with ASN 193 to that of Carbonyl of TZD is about 1.89 Å only. Further *in-silico* pharmacokinetic parameters of these compounds were predicted and found to possess druglike properties for potential oral anti-diabetic and anti-obesity agents.

Acknowledgement: Authors are thankful to management of Indira College of Pharmacy, Pune, for providing necessary facilities and support.

Conflict of Interest: Authors have no conflict of interest.

REFERENCES:

- 1. Alonso A, Sasin J, Bottini N, Friedberg I, Friedberg I, Osterman A, Godzik A, Hunter T, Dixon J, Mustelin T. Protein tyrosine phosphatases in the human genome. Cell. 2004 Jun 11;117(6):699-711.
- 2. Barford D. Molecular mechanisms of the protein serine/threonine phosphatases. Trends in biochemical sciences. 1996 Nov 1;21(11):407-12.
- Barford D, Flint AJ, Tonks NK. Crystal structure of human protein tyrosine phosphatase 1B. Science. 1994 Mar 11;263(5152):1397-404.
- 4. Barr AJ. Protein tyrosine phosphatases as drug targets: strategies and challenges of inhibitor development. Future medicinal chemistry. 2010 Oct 1;2(10):1563-76.
- 5. Combs AP. Recent advances in the discovery of competitive protein tyrosine phosphatase 1B inhibitors for the treatment of diabetes, obesity, and cancer. Journal of medicinal chemistry. 2010 Mar 25;53(6):2333-44.
- Daina A, Michielin O, Zoete V. Swiss ADME: a free web tool to evaluate pharmacokinetics, drug-likeness and medicinal chemistry friendliness of small molecules. Scientific reports. 2017 Mar 3;7(1):42717.
- 7. DeDecker BS. Allosteric drugs: thinking outside the active-site box. Chemistry & Biology. 2000 May 1;7(5):R103-7.
- Dubé N, Tremblay ML. Involvement of the small protein tyrosine phosphatases TC-PTP and PTP1B in signal transduction and diseases: from diabetes, obesity to cell cycle, and cancer. Biochimica et Biophysica Acta (BBA)-Proteins and Proteomics. 2005 Dec 30;1754(1-2):108-17.
- 9. Elchebly M, Payette P, Michaliszyn E, CromLish W, Collins S, Loy AL, Normandin D, Cheng A, Himms-Hagen J, Chan CC, Ramachandran C. Increased insulin sensitivity and obesity resistance in mice lacking the protein tyrosine phosphatase-1B gene. Science. 1999 Mar 5;283(5407):1544-8.

- Ertl P, Rohde B, Selzer P. Fast calculation of molecular polar surface area as a sum of fragment-based contributions and its application to the prediction of drug transport properties. Journal of medicinal chemistry. 2000 Oct 5;43(20):3714-7.
- 11. Frangioni JV, Beahm PH, Shifrin V, Jost CA, Neel BG. The nontransmembrane tyrosine phosphatase PTP-1B localizes to the endoplasmic reticulum via its 35 amino acid C-terminal sequence. Cell. 1992 Feb 7;68(3):545-60
- 12. Friesner RA, Murphy RB, Repasky MP, Frye LL, Greenwood JR, Halgren TA, Sanschagrin PC, Mainz DT. Extra precision glide: Docking and scoring incorporating a model of hydrophobic enclosure for protein— ligand complexes. Journal of medicinal chemistry. 2006 Oct 19;49(21):6177-96.
- 13. Hardy JA, Wells JA. Searching for new allosteric sites in enzymes. Current opinion in structural biology. 2004 Dec 1;14(6):706-15.
- 14. Greenwood JR, Calkins D, Sullivan AP, Shelley JC. Towards the comprehensive, rapid, and accurate prediction of the favorable tautomeric states of drug-like molecules in aqueous solution. Journal of computer-aided molecular design. 2010 Jun;24(6):591-604.
- 15. Klaman LD, Boss O, Peroni OD, Kim JK, Martino JL, Zabolotny JM, Moghal N, Lubkin M, Kim YB, Sharpe AH, Stricker-Krongrad A. Increased energy expenditure, decreased adiposity, and tissue-specific insulin sensitivity in protein-tyrosine phosphatase 1B-deficient mice. Molecular and cellular biology. 2000 Aug
- Krishnan N, Koveal D, Miller DH, Xue B, Akshinthala SD, Kragelj J, Jensen MR, Gauss CM, Page R, Blackledge M, Muthuswamy SK. Targeting the disordered C terminus of PTP1B with an allosteric inhibitor. Nature chemical biology. 2014 Jul;10(7):558-66.
- Krishnan N, Krishnan K, Connors CR, Choy MS, Page R, Peti W, Van Aelst L, Shea SD, Tonks NK. PTP1B inhibition suggests a therapeutic strategy for Rett syndrome. The Journal of clinical investigation. 2015 Aug 3;125(8):3163-77.
- 18. Lee S, Wang Q. Recent development of small molecular specific inhibitor of protein tyrosine phosphatase 1B. Medicinal research reviews. 2007 Jul;27(4):553-73. Lipinski CA, Lombardo F, Dominy BW, Feeney PJ. Experimental and computational approaches to estimate solubility and permeability in drug discovery and development settings. Advanced drug delivery reviews. 1997 Jan 15;23(1-3):3-25.
- 19. Lotfi B, Mebarka O, Alhatlani BY, Abdallah EM, Kawsar SM. Pharmacoinformatics and Breed-Based De Novo Hybridization Studies to



- Develop New Neuraminidase Inhibitors as Potential Anti-Influenza Agents. Molecules. 2023 Sep 18;28(18):6678.
- Montalibet, J.; Kennedy, B. P. Drug Discovery Today Ther. Strateg. 2005, 2, 129. 3. Zhang, S.; Zhang, Z. Drug Discovery Today 2007, 12, 373.
- 21. Najjar A, Olğaç A, Ntie-Kang F, Sippl W. Fragment-based drug design of nature-inspired compounds. Physical Sciences Reviews. 2019 Sep 25;4(9):20180110.
- Nichols AJ, Mashal RD, Balkan B. Toward the discovery of small molecule PTP1B inhibitors for the treatment of metabolic diseases. Drug development research. 2006 Jul;67(7):559-66.
- 23. Patel AD, Pasha TY, Lunagariya P, Shah U, Bhambharoliya T, Tripathi RK. A library of thiazolidin-4-one derivatives as protein tyrosine phosphatase 1B (PTP1B) inhibitors: an attempt to discover novel antidiabetic agents. ChemMedChem. 2020 Jul 3;15(13):1229-42.
- 24. Patel HM, Shaikh M, Ahmad I, Lokwani D, Surana SJ. BREED based de novo hybridization approach: Generating novel T790M/C797S-EGFR tyrosine kinase inhibitors to overcome the problem of mutation and resistance in non small cell lung cancer (NSCLC). Journal of Biomolecular Structure and Dynamics. 2021 May 24;39(8):2838-56.
- 25. Pattan, Shashikant R., Prajact Kekare, Ashwini Patil, Ana Nikalje, and B. S. Kittur. "Studies on the synthesis of novel 2, 4-thiazolidinedione derivatives with antidiabetic activity." (2009): 225-230.
- 26. Shivakumar D, Williams J, Wu Y, Damm W, Shelley J, Sherman W. Prediction of absolute solvation free energies using molecular dynamics free energy perturbation and the OPLS force field. Journal of chemical theory and computation. 2010 May 11;6(5):1509-19.
- 27. Singh G, Singh R, Monga V, Mehan S. 3, 5-Disubstituted-thiazolidine-2, 4-dione hybrids as antidiabetic agents: Design, synthesis, in-vitro and In vivo evaluation. European Journal of Medicinal Chemistry. 2024 Feb 15;266:116139.
- 28. Tonks, N. K., Diltz, C., & Fischer, E. Purification of the major protein-tyrosine-phosphatases of human placenta. The Journal of Biological Chemistry. 1988 263(14), 6722–6730.
- 29. Vistoli G, Pedretti A, Testa B. Assessing drug-likeness—what are we missing?. Drug discovery today. 2008 Apr 1;13(7-8):285-94.
- Wiesmann C, Barr KJ, Kung J, Zhu J, Erlanson DA, Shen W, Fahr BJ, Zhong M, Taylor L, Randal M, McDowell RS. Allosteric inhibition of protein tyrosine phosphatase 1B. Nature structural & molecular biology. 2004 Aug 1;11(8):730-7.

- Zabolotny JM, Bence-Hanulec KK, Stricker-Krongrad A, Haj F, Wang Y, Minokoshi Y, Kim YB, Elmquist JK, Tartaglia LA, Kahn BB, Neel BG. PTP1B regulates leptin signal transduction in vivo. Developmental cell. 2002 Apr 1;2(4):489-95.
- 32. Zhang ZY. Protein tyrosine phosphatases: prospects for therapeutics. Current opinion in chemical biology. 2001 Aug 1;5(4):416-23.
- 33. Zhang ZY. Drugging the undruggable: therapeutic potential of targeting protein tyrosine phosphatases. Accounts of chemical research. 2017 Jan 17;50(1):122-9.
- 34. Zhang ZY, Lee SY. PTP1B inhibitors as potential therapeutics in the treatment of type 2 diabetes and obesity. Expert opinion on investigational drugs. 2003 Feb 1;12(2):223-33.
- 35. Zhong H, Tran LM, Stang JL. Induced-fit docking studies of the active and inactive states of protein tyrosine kinases. Journal of Molecular Graphics and Modelling. 2009 Nov 1;28(4):336-46.
- 36. Zhu K, Borrelli KW, Greenwood JR, Day T, Abel R, Farid RS, Harder E. Docking covalent inhibitors: a parameter free approach to pose prediction and scoring. Journal of chemical information and modeling. 2014 Jul 28;54(7):1932-40.